Research Journal of Applied Sciences 9 (1): 37-43, 2014
ISSN: 1815-932X

Prediction and Development of Mathematical Models on Super Duplex Stainless Steel Weld Clad by FCAW

[1]A.V. Balan and [2]T. Kannan
[1]Department of Mechanical Engineering, KSR College of Engineering, 637215 Tiruchengode, Tamilnadu, India
[2]Department of Mechanical Engineering, SVS College of Engineering, Coimbatore, Tamilnadu, India

Abstract: Generally, the quality of a weld cladding is directly influenced by the welding input parameter settings. Selection of proper process parameters is important to obtain the desired weld bead profile and quality. Corrosion is the tendency of a metal to return to its most stable thermodynamics state with the most negative free energy of formation. Most simply stated, it is a chemical reaction of the metal with the environment to form an oxide, nitride, carbonate, sulphate or other stable compound. This study addresses the modeling parameters in FCAW process using set of experimental data and multiple regression analysis. The input process variables considered here include wire feed rate (F), welding speed (S), nozzle to plate distance (N) and weld gun angle (T) each having five levels. The process output characteristics are weld bead width (W), height of reinforcement (R) and depth of penetration (P). The regression modeling is used in order to establish the relationships between input and output parameters. In this research work, the developed models were examined for their adequacy. The result shows that the models can predict the weld bead geometry with reasonable accuracy.

Key words: Cladding, bead geometry, Flux Cored Arc Welding (FCAW), mathematical models, feed rate

INTRODUCTION

Materials include stainless steel, inconel and monel are deposited on carbon and low alloy steels to improve the corrosion resistance, in applications like nuclear power generating components, chemical vessels, etc. (Alam *et al*., 2002). Apart from this, buildup is also done to reclaim worn-out components made of costly materials. Thus, buildup of materials forms a cost effective materials maintenance tool which saves time and effort on procurement. Several welding processes are successfully applied for building up the material. The welding techniques normally employed are fusion welding techniques such as Gas Metal Arc Welding (GMAW), Manual Metal Arc Welding (MMAW), Flux Cored Arc Welding (FCAW), Submerged Arc Welding (SAW), Electro Slag Welding (ESW), Plasma Arc Welding (PAW) and explosive welding (Cary and Helzer, 2005). Among the fusion welding processes, Flux Cored Arc Welding (FCAW) had been widely used for cladding (Cheremisinoff, 1987) due to several advantages such as simpler and more adaptable than SAW, high deposition rates, less operator skill required than GMAW, less fume generation, reduced distortion compared to SMAW (Cochran and Cox, 1957, 1963). Corrosion is an obstacle which weakens the steel structure causing its failure. Though corrosion cannot be eliminated fully, it can be reduced to certain extent. Corrosion resistance protective layer is formed over the less corrosion-resistant substrate by a process called weld cladding (Cornu, 1988). The bead geometry as shown in Fig. 1.

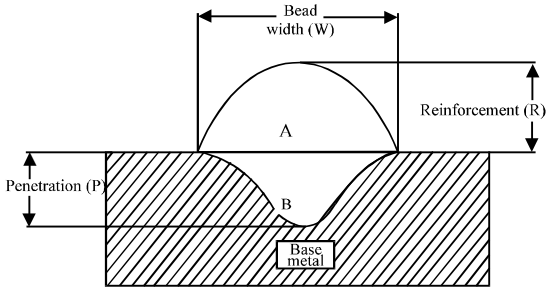

Fig. 1: Bead geometry

Corresponding Author: A.V. Balan, Department of Mechanical Engineering, KSR College of Engineering, 637215 Tiruchengode, Tamilnadu, India

Table 1: Chemical composition of base metal and filler wire

	Elements (wt. %)											
Materials	C	Mn	Si	S	P	Cr	Ni	Mo	Cu	N	Fe	Al
Mild steel IS2062	0.196	1.12	0.293	0.011	0.0044	0.128	0.0336	0.0275	0.0963	-	98.02	0.064
Filler wire FC2507	0.027	0.64	0.470	0.005	0.0180	25.30	8.6200	4.3600	0.0600	0.28	-	-

Fig. 2: Experimental setup

Inadequate weld bead dimensions or depth of penetration may contribute to failure of a welded structure since penetration determines the percentage dilution of the deposited metal. To avoid such occurrences, the input or welding process variables which influence the weld bead penetration must therefore be properly selected and optimized to obtain an acceptable weld bead penetration and hence the composition of the weld metal matches that of the deposited on. This investigation is based on a central composite rotatable design technique that had been used to develop a mathematical model correlating the four welding process variables of wire feed rate (F), welding speed (S), nozzle to plate distance (N) and weld gun angle (T) to the weld bead parameters in Flux Cored Arc Welding (FCAW). The requirements are base material as mild steel IS2062, deposited material as super duplex stainless steel FC2507, shielding gas as mixture of argon (80%) and CO_2 (20%) and welding process as a Flux Cored Arc Welding (FCAW). Experiments were conducted based on four-factors, five-level central composite rotatable design with full replication technique.

Experiment details: The experiments were conducted by using Lincoln Electric PRO V350. Test pieces of size 300×200×20 mm were cut from low carbon structural steel (IS: 2062) plate and their surfaces were ground to remove oxide scale and dirt before the cladding process. Super duplex stainless steel filler wire (FC2507) of 1.2 mm diameter was used for depositing the weld beads. Chemical composition of the base metal and filler wire is given in Table 1. Gas mixture of 80% argon and 20% of CO_2 was used for shielding. The experimental setup used consisted of a traveling carriage with a table for supporting the specimens as shown in Fig. 2.

The welding gun was held stationary in a frame mounted above the worktable and it was provided with an attachment for both up-down and angular movements for setting the required welding gun angle (T) and nozzle to plate distance (N), respectively. The experiments were conducted by laying single bead using stringer bead technique.

MATERIALS AND METHODS

The step by step experimental design procedures used for this study are briefly explained.

Identification of input process parameters and response variables: The input process parameters were wire feed rate (F), nozzle to plate distance (N), welding speed (S) and welding gun angle (T). The chosen responses were bead width (W), height of reinforcement (R) and depth of penetration (P).

Finding working ranges of input process parameters: The working ranges of all selected parameters were fixed by conducting trial runs. This was carried out by varying one of the parameters while keeping the rest of them at constant values (Gunaraj and Murugan, 1999). The working range of each parameter was decided upon by inspecting the weld bead for a smooth appearance and the absence of visible defects such as undercut, surface porosity, etc. The upper limit of the parameter was coded as +2 and the lower limit was coded as -2. The coded values were used as intermediate values which can be calculated using the following Eq. 1:

$$X_i = 2\frac{[2X-(X_{max}+X_{min})]}{(X_{max}-X_{min})} \quad (1)$$

Where:

X_i = The required coded value of a parameter X
X = Any value of the parameter from X_{min} to X_{max}
X_{min} = The lower limit of the parameter
X_{max} = The upper limit of the parameter

The chosen levels of the selected process parameters with their units and notations are given in Table 2.

Table 2: Chosen welding process parameters and their levels

			Factor levels				
Parameters	Units	Notation	-2	-1	0	+1	+2
Wire feed rate	inch/min	F	150	175	200	225	250
Welding speed	mm/min	S	100	120	140	160	180
Nozzle to plate distance	mm	N	16	18	20	22	24
Welding gun angle	Degree (°)	T	90	100	110	120	130

Table 3: Design matrix and the observed values of weld bead parameters

Trial No.	F	S	N	T	W (mm)	R (mm)	P (mm)
1	-1	-1	-1	-1	8.3851496	4.1305480	0.3716020
2	1	-1	-1	-1	9.7668334	4.6194980	0.4202684
3	-1	1	-1	-1	8.0474820	3.3771840	0.3764534
4	1	1	-1	-1	8.4300060	3.7886640	0.4432808
5	-1	-1	1	-1	8.5199220	4.2724070	0.3271520
6	1	-1	1	-1	10.0971350	4.7753270	0.3784854
7	-1	1	1	-1	8.4963000	3.6888420	0.3423412
8	1	1	1	-1	8.9969340	3.9284910	0.3792220
9	-1	-1	-1	1	8.6995000	3.9629080	0.3303270
10	1	-1	-1	1	10.1234240	4.1588690	0.4077716
11	-1	1	-1	1	8.5247734	3.3666430	0.3384550
12	1	1	-1	1	8.6093300	3.6231830	0.4319016
13	-1	-1	1	1	8.9261950	3.9966900	0.3186684
14	1	-1	1	1	10.2876350	4.6868334	0.3625850
15	-1	1	1	1	8.6672420	3.5093910	0.3300730
16	1	1	1	1	9.6116140	3.8745160	0.3638550
17	-2	0	0	0	7.7175360	3.7449760	0.3272790
18	2	0	0	0	10.0041710	4.0971470	0.5506720
19	0	-2	0	0	10.1348540	4.8378110	0.4196334
20	0	2	0	0	8.1671160	3.4072830	0.4984750
21	0	0	-2	0	7.7461110	3.1629350	0.8342630
22	0	0	2	0	9.6149414	4.0995600	0.2674620
23	0	0	0	-2	8.9293700	3.7744400	0.3776980
24	0	0	0	2	9.7896934	3.5298380	0.1789430
25	0	0	0	0	8.4349590	3.8750494	0.7073900
26	0	0	0	0	7.8691740	3.8748970	0.7073900
27	0	0	0	0	8.4476590	4.2840910	0.7073900
28	0	0	0	0	8.4349590	3.8694360	0.7073900
29	0	0	0	0	8.4476590	3.8748970	0.5295900
30	0	0	0	0	8.4476590	3.8694360	0.7073900
31	0	0	0	0	8.4349590	3.8694360	0.7073900

Development of design matrix: The design matrix chosen to conduct the experiments was a central composite rotatable design. This design matrix (Harris and Smith, 1983) comprised a full replication of 2^4 (=16) factorial design plus seven center points and eight star points which is given in Table 3. All welding parameters at the intermediate levels (0) constituted the center points and the combination of each welding parameters at either its highest value (+2) or its lowest value (-2) with the other three parameters of the intermediate levels (0) constituted the star points. Thus, the 31 experimental runs allowed the estimation of linear, quadratic and two-way interactive effects of the process parameters on clad bead geometry.

Conducting experiments as per the design matrix: The experiments were conducted at Welding Research Center at Kumaraguru College of Technology, Coimbatore. In this research, 31 deposits were made using cladding conditions corresponding to each treatment combination of parameters as shown in Table 3 at random. At the end of each run, settings for all four parameters were disturbed and reset for the next deposit. That was essential to introduce variability caused by errors in experimental settings (Juffus, 1999).

Recording the response variables: Transverse sections of each weld overlay was cut using power hacksaw from mid length position of the welds and the end faces were machined accurately. These specimens were prepared by the usual metallurgical polishing methods and etched with 5% nital solution. The weld bead profiles were traced using a reflective type optical profile projector at a magnification of 10. The profile images were imported to AutoCAD 2004 Software as raster image and profiles were traced in 2D form. From the 2D diagram, height of reinforcement, the depth of penetration, weld bead width and penetration and reinforcement were measured. The observed values of weld bead width, depth of penetration, height of reinforcement for 31 trials are given in the Table 3.

Calculation of regression coefficients and development of mathematical models: The response function representing any of the weld bead parameters can be expressed by using Eq. 2:

$$Y = f(X_1, X_2, X_3, X_4) \quad (2)$$

Where:

Y = The response (e.g., weld bead width)
X_1 = The wire feed rate (F)
X_2 = The welding speed (S)
X_4 = The welding gun angle (T)
X_3 = The Nozzle to plate distance (N)

The second order response surface model for the four factors is given in Eq. 3:

$$Y = \beta_0 + \sum_{i=1}\beta_i X_i + \sum_{i=1}\beta_{ii} X_i^2 \sum_{i=1, i<j}\beta_{ij} X_i X_j \quad (3)$$

The second order response surface model (Eq. 3) can be expressed as follows:

$$\begin{aligned} Y = {} & \beta_0 + \beta_1 X_1 + \beta_2 X_2 + \beta_3 X_3 + \beta_4 X_4 + \beta_{11} X_1^2 + \beta_{22} X_2^2 + \\ & \beta_{33} X_3^2 + \beta_{44} X_4^2 + \beta_{12} X_1 X_2 + \beta_{13} X_1 X_3 + \beta_{14} X_1 X_4 + \\ & \beta_{23} X_2 X_3 + \beta_{24} X_2 X_4 + \beta_{34} X_3 X_4 \end{aligned} \quad (4)$$

where, β_0 is the free term of the regression equation, the coefficients β_1, β_2, β_3 and β_4 are the linear terms, the coefficients β_{11}, β_{22}, β_{33} and β_{44} are quadratic terms and the coefficients β_{12}, β_{13}, β_{14}, β_{24} and β_{34} are interaction terms (Khuri and Cornell, 1996; Kumar and Sundarrajan, 2009; Montgomery, 2001; Montgomery and Runger, 1999; Murugan and Parmar, 1994, 1995).

The regression coefficients were also calculated by using Quality America Six Sigma Software (DOE-PC-IV) and the same were verified using Minitab16 Software. After determining the coefficients, mathematical models were developed. The developed models with welding parameters in coded form are given:

Bead width (W) (mm) = 8.36+0.51×F- 0.39×S+0.281×N+0.185×T+0.125×F×F+0.198×S×S+0.08×N×N+0.25×T×T-0.24×F×S+0.069×F×N-0.002×F×T+0.082×S×N+0.011×S×T+0.003×N×T

Height of reinforcement (R) (mm) = 3.931+0.161×F-0.346×S+0.149×N-0.079×T+0.023×F×F+0.073×S×S-0.049×N×N-0.044×T×T-0.038×F×S+0.028×F×N-0.008×F×T-0.001×S×N+0.036×S×T+0.013×N×T

Depth of penetration (P) (mm) = 0.682+0.037×F+0.01×S-0.06×N-0.023×T-0.071×F×F-0.066×S×S-0.043×N×N-0.111×T×T+0.001×F×S-0.008×F×N+0.003×F×T-0.002×S×N+0×S×T+0.003×N×T

The insignificant coefficients were eliminated without affecting the accuracy of the developed models by using t-test. This was done by using back elimination technique, available in Quality America Six Sigma Software (DOE-PC-IV). The final mathematical models were constructed by using only significant coefficients. The developed final models with welding parameters in coded form are given:

Bead width (W) (mm) = 8.360+0.510×F-0.390×S+0.281×N+0.185×T+0.125×F×F+0.198× S×S+0.080×N×N+0.250×T×T-0.240×F×S+0.069×F×N +0.082×S×N

Height of reinforcement (R)(mm) = 3.955+0.161×F-0.346×S+0.149×N-0.079×T+0.071×S×S-0.052×N×N-0.047×T×T

Depth of penetration (P) (mm) = 0.682+0.037×F -0.060×N-0.023×T-0.071×F×F-0.066×S×S-0.043×N×N-0.111×T×T

Checking the adequacy of the developed models: The adequacy of the developed models were tested using the analysis of variance technique (Raja *et al*., 1999). That include the calculated values of F-ratio of the developed model which did not exceed the standard tabulated value of F-ratio for a desired level of confidence (say 95%) and if the calculated value of R-ratio of the developed model exceeded the standard tabulated value of R-ratio for a desired level of confidence (say 95%) then the models might be considered adequate within the confidence limit. It is found from Table 4 that all models are adequate. The validity of these models were again tested by drawing scatter diagrams as shown in Fig. 3-5 which showed the observed and predicted values of weld bead geometry.

Table 4: Analysis of variance for testing adequacy of the models

	First order terms		Second order terms		Lack of fit		Error terms				
Bead geometry	SS	df	SS	df	SS	df	SS	df	F-ratio	R-ratio	Adequacy of the models
Bead width (W)	12.599	4	3.957	10	0.727	10	0.281	6	1.554	25.268	Adequate
Depth of penetration (P)	0.137	4	0.538	10	0.114	10	0.027	6	2.515	10.673	Adequate
Height of reinforcement (R)	4.177	4	0.391	10	0.347	10	0.145	6	1.429	13.457	Adequate

F-ratio (10, 6, 0.05) = 4.09; R-ratio (14, 6, 0.05) = 3.96; SS = Sum of Squares; df = degrees of freedom

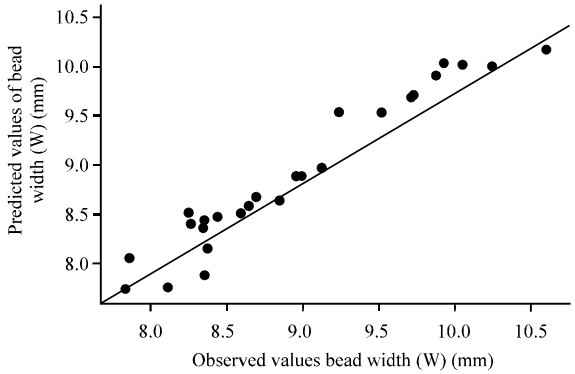

Fig. 3: Scatter diagram of bead widh model (W)

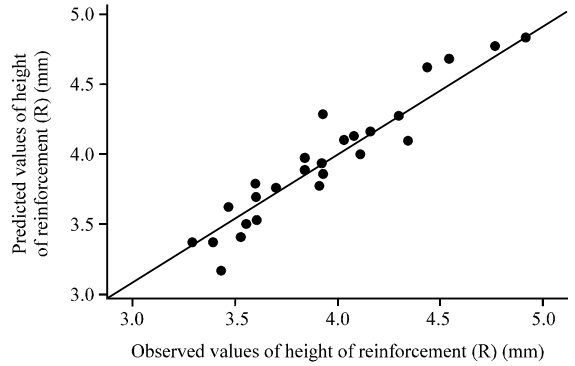

Fig. 4: Scatter diagram of Reinforcement Model (R)

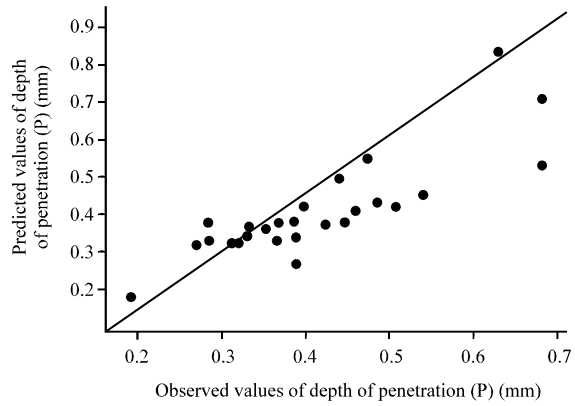

Fig. 5: Scatter diagram of depth Penetration Model (P)

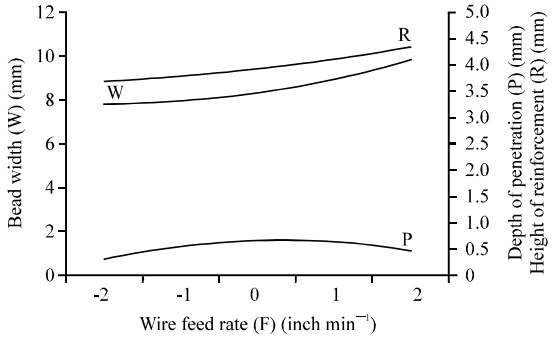

Fig. 6: Direct effect of wire feed rate (F) on clad bead geometry

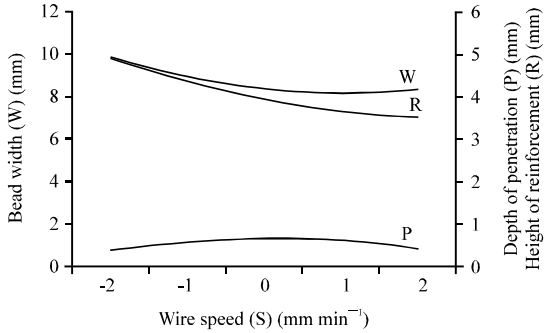

Fig. 7: Direct effect of welding speed (S) on clad bead geometry

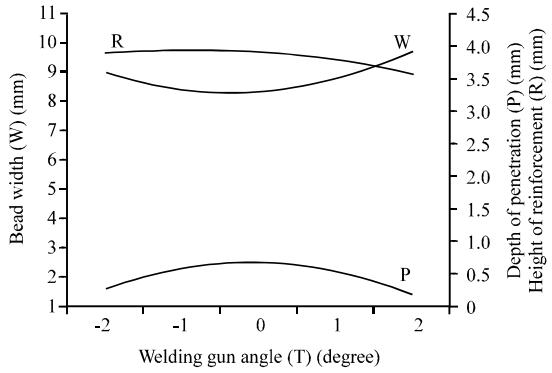

Fig. 8: Direct effect of welding gun angle (T) on clad bead geometry

RESULTS AND DISCUSSION

The mathematical models developed can be employed to predict the clad bead geometry for the range of parameters used in this investigation by substituting their respective values in coded form. Based on these models, the effect of process parameters on clad bead geometry were studied and shown in the Fig. 6-9.

Direct effect of process parameters on clad bead geometry

Direct effect of wire feed rate (F) on clad bead geometry: From Fig. 6, it can be perceived that with all other variables kept constant, the rise of wire feed rate increases depth of penetration, height of reinforcement and weld bead width. This can be attributed to the fact that increase in wire feed rate increases the welding current resulting in

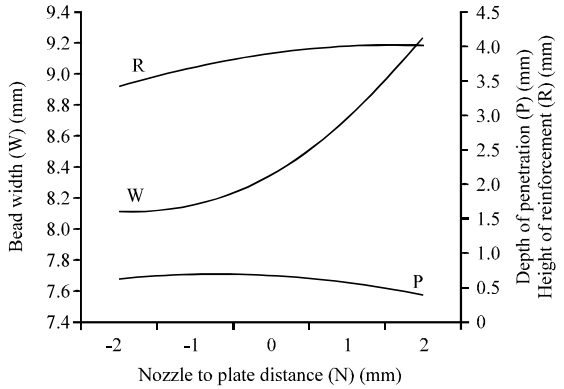

Fig. 9: Direct effect of nozzel to plate distance (N) on clad bead geometry

a higher current density, better power per unit length of the weld bead and initiating larger volume of the base metal to melt for deeper penetration.

Direct effect of welding speed (S) on clad bead geometry: From Fig. 7, it can be concluded that increase in welding speed decreases height of reinforcement and width of weld bead. As the welding speed increases, it causes reduced heat input per unit length of weld bead and less filler metal is applied per unit length of the weld (Rieber, 1985). The depth of penetration decreases with decrease in welding speed. At low welding speed, the effect of arc is reduced by the formation of weld pool cushioning due to the vertical arc and hence prevents deeper penetration.

Direct effect of welding gun angle (T) on clad bead geometry: From Fig. 8, it is evident that depth of penetration, height of reinforcement decreases gradually and welds bead width increases with the increase in welding gun angle. In backhand welding (i.e., gun angle >90°) when the gun angle is increased, the molten metal flows under the arc, results in reduced penetration, height of reinforcement and weld bead width increases.

Direct effect of nozzle to plate distance (N) on clad bead geometry: It is evident from Fig. 9 that depth of penetration decreases slightly with increase in nozzle to plate distance but weld bead width and height of reinforcement increase with increase in nozzle to plate distance. Increase in nozzle to plate distance increases the circuit resistance which reduces the welding current. This lowers the heat input per unit length of the weld with a consequent reduction in fusion area. Hence, the depth of penetration is decreased. Also, with increase in nozzle to plate distance, the arc length is increased. Hence, the bead width is increased due to wider arc area at the weld surface. This consequently increases the reinforcement height because the same volume of filler metal is added (Walpole and Myers, 1998).

CONCLUSION

Based on the central composite rotatable design technique, the developed mathematical model was designed by using a five-level, four-factor full-factorial design matrix to predict the clad bead geometry like Weld bead width (W), height of reinforcement (R) and depth of penetration (P) for super duplex stainless steel cladding deposited by Flux Cored Arc Welding (FCAW). The predicted results obtained from mathematical models are closely related to experimental results. The bead geometry includes depth of penetration (P), height of reinforcement (R) and weld bead width (W) increases in wire feed rate. Weld bead width (W) and height of reinforcement (R) and depth of penetration (P) decrease with the increase in welding speed. Depth of penetration, height of reinforcement decrease gradually and weld bead width increases with the increase in welding gun angle using back hand angle (i.e., gun angle >90°). Weld bead width (W) and height of reinforcement (R) increase with increase in nozzle to plate distance and depth of penetration decreases.

REFERENCES

Alam, N., L. Jarvis and D. Harris, 2002. Laser cladding for repair of engineering components. Aust. Welding J., 47: 38-47.

Cary, H.B. and S.C. Helzer, 2005. Modern Welding Technology. Pearson/Prentice Hall, New Jersey, ISBN: 9780131130296, Pages: 316.

Cheremisinoff, N.P., 1987. Practical Statistics for Engineers and Scientists. Technomic Publishing Company, Inc., Lancaster, PA.

Cochran, W.G. and G.M. Cox, 1957. Experimental Designs. 2nd Edn., John Wiley and Sons, New York.

Cochran, W.G. and G.M. Cox, 1963. Experimental Designs. 2nd Edn., John Wiley and Sons, Inc., New York, Pages: 613.

Cornu, J., 1988. Advanced Welding Systems. Vol. 2, IFS, Publications Ltd., UK.

Gunaraj, V. and N. Murugan, 1999. Prediction and comparison of the area of the heat-affected zone for the bead-on-plate and bead-on-joint in submerged arc welding of pipes. J. Mater. Process. Technol., 95: 246-261.

Harris, P. and B.L. Smith, 1983. Factorial techniques for weld quality prediction. Metal Constr., 15: 661-666.

Juffus, L., 1999. Welding Principles and Applications. 4th Edn., Delmar Publishers, New York.

Khuri, A.I. and J.A. Cornell, 1996. Response Surfaces, Designs and Analyses. 2nd Edn., Marcell Dekker, Inc., New York.

Kumar, A. and S. Sundarrajan, 2009. Effect of welding parameters on mechanical properties and optimization of pulsed TIG welding of Al-Mg-Si alloy. Int. J. Adv. Manuf. Technol., 42: 118-125.

Montgomery, D.C. and G.C. Runger, 1999. Applied Statistics and Probability for Engineers. 2nd Edn., John Wiley and Sons, New York.

Montgomery, D.C., 2001. Design and Analysis of Experiments. 5th Edn., John Wiley and Sons, New York.

Murugan, N. and R.S. Parmar, 1994. Effects of MIG process parameters on the geometry of the bead in the automatic surfacing of stainless steel. J. Mater. Process. Technol., 41: 381-398.

Murugan, N. and R.S. Parmar, 1995. Effects of MIG process parameters on the geometry of the bead in the automatic surfacing of stainless steel. Int. J. Join. Mater., 7: 71-80.

Raja, A., K.L. Rohira and S. Samidas, 1999. Flux cored arc welding-selection of consumables, equipment's and applications. WRI J., 20: 124-129.

Rieber, F., 1985. Hand Book of welding. PWS-KENT Publishing Company, USA.

Walpole, R.E. and R.H. Myers, 1998. Probability and Statistics for Engineers and Scientists. 6th Edn., Prentice Hall, Upper Saddle River, NJ.